

# Distributed Reactive Power Control based Conservation Voltage Reduction in Active Distribution Systems

Selcuk EMIROGLU<sup>1</sup>, Yilmaz UYAROGLU<sup>1</sup>, Gulcihan OZDEMIR<sup>2</sup>

<sup>1</sup>Department of Electrical and Electronics Engineering, Sakarya University, Sakarya, 54100, Turkey

<sup>2</sup>Informatics Institute, Istanbul Technical University, Istanbul, 34469, Turkey

selcukemiroglu@sakarya.edu.tr

**Abstract**—This paper proposes a distributed reactive power control based approach to deploy Volt/VAr optimization (VVO) / Conservation Voltage Reduction (CVR) algorithm in a distribution network with distributed generations (DG) units and distribution static synchronous compensators (D-STATCOM). A three-phase VVO/CVR problem is formulated and the reactive power references of D-STATCOMs and DGs are determined in a distributed way by decomposing the VVO/CVR problem into voltage and reactive power control. The main purpose is to determine the coordination between voltage regulator (VR) and reactive power sources (Capacitors, D-STATCOMs and DGs) based on VVO/CVR. The study shows that the reactive power injection capability of DG units may play an important role in VVO/CVR. In addition, it is shown that the coordination of VR and reactive power sources does not only save more energy and power but also reduces the power losses. Moreover, the proposed VVO/CVR algorithm reduces the computational burden and finds fast solutions. To illustrate the effectiveness of the proposed method, the VVO/CVR is performed on the IEEE 13-node test system feeder considering unbalanced loading and line configurations. The tests are performed taking the practical voltage-dependent load modeling and different customer types into consideration to improve accuracy.

**Index Terms**—energy conservation, reactive power control, renewable energy sources, smart grids, voltage control.

## I. INTRODUCTION

VVO on operation and control of electric distribution power systems draws much more attention in recent years as a significant tool to improve energy efficiency. VVO is mainly employed to obtain a better voltage profile and optimal reactive power flow control in distribution systems. The coordination between the VVO devices (switched shunt capacitors, load tap changer (LTC), VR and DG) is provided by the objective function and system operating constraints [1].

In addition to the loss reduction and voltage profile improvement as objectives of VVO, it also provides a significant tool for the distribution system called CVR. The CVR aims to reduce demand to improve efficiency of the system by decreasing the voltage magnitudes down to the minimum allowable limits without affecting the performance of the end user's devices [2]. Also, CVR should ensure the international standards such as ANSI.

This work was supported by the Scientific and Technological Research Council of Turkey (TUBITAK) BIDEB-2214 research fellowship programme and Research Fund of the Sakarya University.

Based on the standards, the limits are defined not to affect adversely the usage and the performance of customer loads or devices [3].

CVR has been widely tested and employed by variety of utilities in many countries. It has been shown that utilities and the system adopting CVR saves considerable energy and hence contributes the economy [4]. Dominion Virginia Power Co reported a saving ~2.8% of annual energy [5]. The Snohomish County PUD has obtained 53,856 MWh/yr energy saving in addition to reduced distribution system losses (11,226 MWh/yr) and achieved improved voltage profile [6]. Ireland has saved 1.7% energy with 1% voltage reduction by deploying CVR technology to distribution feeders [7]. It has been reported that the deployment of CVR on residential circuits in Australia provided a 1% energy saving with 2.5% voltage reduction [7]. Idaho Power reported that an energy saving between 0.9-1.8% for a typical customer is obtained [8]. Northeast Utilities applied the CVR to 32 high voltage distribution circuits by reducing the voltage 1% and resulting in a 1% reduction in energy consumption [9]. Also Hydro Quebec (HQ) reported that ~1.5TWh (0.4%) reduction in energy consumption by 1% voltage reduction is obtained when CVR is adopted [10].

Recently, the nature of distribution network has been changed from a passive distribution network to active one by deploying the DGs [11]. The DGs are installed nearby the load centers to reduce the losses and carbon emissions and to improve the reliability and efficiency of a system. Integration of DGs to power distribution system poses a great challenge such as protection, power quality and voltage regulation [12].

However, the increasing penetration of distributed generation (DG) changes the feeder voltage profiles, which greatly affect the VVO in distribution systems due to the highly variable and intermittent outputs of renewable generation. Moreover, distribution system operation may have been deteriorated by massive integration of DGs due to reverse power flow from the distribution system in terms of VVO. Therefore, it is essential to consider the impact of DGs on power systems [3],[13].

The effect of DG penetration on CVR is investigated in [13] which presented that a small amount of DG penetration provides smooth voltage profile in result of larger energy and economic savings. However, the reactive power capability of DG and its impact is not taken under consideration. Thus, when the active distribution network is

properly planned and regulated, DGs could improve the voltage profile along the feeder and could reduce the power losses on a distribution network by providing active and reactive power support. Accordingly, it provides improved efficiency and better economics if they are controlled appropriately.

Traditionally, DGs are not permitted to inject the reactive power to the grid under the current regulation in many countries [14]. However, there have been many suggestions to change standards such as allowing the reactive power support from the inverter based DGs [15].

Optimal control of the reactive power by controlling the inverters of photovoltaic (PV) units was proposed in [16]. Also, References [17-18] show that the reactive power capability of inverter based DGs can be utilized for VVO.

Recently, several optimization approaches such as linear programming and gradient-based algorithms for VVO have been applied to the distribution systems [19-21]. But, the VVO is a highly nonlinear and discrete optimization problem due to nonlinearity of power flow equations and discrete variables. The optimal control and coordinating of all VVO devices are difficult to solve with using traditional optimization methods due to the complexity and heavy computational burden and hence it is time consuming [22]. Therefore, these conventional techniques may not be suitable for solving the problem effectively [22-23].

Balanced network model is used a number of studies to solve the VVO problem [1-2], [24]. Power distribution systems, however, are naturally unbalanced since they contain unbalanced three phase, single and two phase feeders and laterals providing powers to customers through unbalanced line configurations with different unbalance loading levels of phases and mutual coupling between two and three phase lines [25].

This paper proposes a two stages VVO/CVR algorithm based on a distributed reactive power algorithm to provide a better voltage profile and minimize power demand in unbalanced power distribution systems with D-STATCOMs and DGs by using the reactive power capability of PV inverters. The study focuses on the control strategy to reduce the power and energy demand ensuring the voltage within the predefined limit by reactive power sources and tap changer transformer.

The CVR problem formulated as a nonlinear optimization problem is solved based on a distributed way in order to reduce the computational burden and to save time. The distributed reactive power controllers are designed based on Lyapunov theory. Then, the tap reference is calculated based on the minimum node voltages to fulfill CVR objective by providing all node voltages within the limits. To obtain reliable control of VVO devices, a voltage-sensitive load model based on typical customers defined with ZIP (constant impedance  $Z$ , constant current  $I$  and constant power  $P$ ) coefficients was used for distribution networks considering the mutual coupling between lines.

## II. PROBLEM FORMULATION

### A. Objective Function

The total power loss in the distribution power system can be calculated by the difference between the total generation

and total load [26]. The objective of active power loss minimization ( $f$ ) is formulated as follows:

$$f = P_{loss} = \sum_{i=1}^n P_{Gi} - \sum_{i=1}^n P_{Li} = \sum_{i=1}^n \sum_{j=1}^n V_i V_j Y_{ij} \cos(\theta_{ij} + \delta_{ji}) \quad (1)$$

where  $P_{Gi}$ ,  $P_{Li}$  are the active power generation and the consumption at node  $i$ , respectively,  $Y_{ij}$  and  $\theta_{ij}$  are the magnitude and angle of admittance between  $i$  and  $j$  nodes,  $V_i$ ,  $V_j$  and  $\delta_{ij} = \delta_i - \delta_j$  are the node voltages and the angles of  $i$  and  $j$  nodes, respectively.

### B. System and Operational Constraints

#### 1) Equality Constraints

Real and reactive power flow equations stand for equality constraints. They are specified as follows.

$$\Delta P_i = P_{Gi} - P_{Li} - V_i \sum_{j=0}^{N_b} V_j (\cos \theta_{ij} G_{ij} + \sin \theta_{ij} B_{ij}) = 0 \quad (2)$$

$$\Delta Q_i = Q_{Gi} - Q_{Li} - V_i \sum_{j=0}^{N_b} V_j (\sin \theta_{ij} G_{ij} - \cos \theta_{ij} B_{ij}) = 0 \quad (3)$$

where  $Q_{Gi}$  and  $Q_{Li}$  are the reactive power generation and load at bus  $i$ .  $G_{ij}$  and  $B_{ij}$  are the real and imaginary part of admittance matrix  $Y_{ij}$  respectively.

#### 2) Inequality Constraints

The inequality constraints include the constraints on both the control and the dependent variables. Inequality constraints define upper and lower bounds on a variable.

-Reactive power limits of D-STATCOMs

$$[Q_{min}] \leq [Q_{D-STATCOM}] \leq [Q_{max}] \quad (4)$$

-Smart inverter limit of PVs

$$[Q_{inv,min}] \leq [Q_{inv}] \leq [Q_{inv,max}] \quad (5)$$

Smart inverter is employed to integrate the PV as a DG. The reactive power output of PV inverter is calculated for every time period based on the active power output of PV and apparent power rating of inverter. The maximum reactive power injection or absorption capacity of inverter can be calculated as follows [24]:

$$Q_{inv,max} = \sqrt{S_{inv}^2 - P_{pv}^2} \quad (6)$$

-Transformer tap settings

$$V_{tap,pv}(t) = 1 + Tap(t) \Delta V_{step} \quad (7)$$

here,  $Tap = [-16, \dots, 0, \dots, 16]$  and  $\Delta V_{step} = 0.00625$

-Node Voltages limit

$$[|V_{min}|] \leq [|V|] \leq [|V_{max}|] \quad (8)$$

### C. Load model

The loads are modeled as a voltage dependent load, to obtain more accurate control for the VVO/CVR. Typically, customer loads consist of the combination of all loads. Hence, the ZIP model developed for residential, commercial and industrial loads is used for the VVO/CVR algorithm.

ZIP parameters are the coefficients of a load model consisting of constant impedance  $Z$ , constant current  $I$  and constant power  $P$  loads.

The polynomial expressions for active and reactive powers of the ZIP coefficients model [13] are:

$$P_{Li} = P_0 \left[ Z_p \left( \frac{V_i}{V_0} \right)^2 + I_p \left( \frac{V_i}{V_0} \right) + P_p \right] \text{ subject to} \quad (9)$$

$$Z_p + I_p + P_p = 1 \quad (10)$$

$$Q_{Li} = Q_0 \left[ Z_q \left( \frac{V_i}{V_0} \right)^2 + I_q \left( \frac{V_i}{V_0} \right) + P_q \right] \text{ subject to} \quad (11)$$

$$Z_q + I_q + P_q = 1 \quad (12)$$

where  $P_{Li}$  and  $Q_{Li}$  are the active and reactive powers at operating voltage ( $V_i$ );  $P_0$  and  $Q_0$  are the active and reactive powers at rated voltage ( $V_0$ );  $Z_p$ ,  $I_p$  and  $P_p$  are the ZIP coefficients for active power;  $Z_q$ ,  $I_q$  and  $P_q$  are the ZIP coefficients for reactive power.

TABLE I. ZIP COEFFICIENTS FOR DIFFERENT CUSTOMER CLASSES [28]

| Class              | $Z_p$ | $I_p$ | $P_p$ | $Z_q$ | $I_q$  | $P_q$ | Node    |
|--------------------|-------|-------|-------|-------|--------|-------|---------|
| <b>Commercial</b>  | 0.43  | -0.06 | 0.63  | 4.06  | -6.65  | 3.59  | 5-9-    |
| <b>Residential</b> | 0.85  | -1.12 | 1.27  | 10.96 | -18.73 | 8.77  | 6-11-12 |
| <b>Industrial</b>  | 0     | 0     | 1     | 0     | 0      | 1     | 4-7     |

In the ZIP model, the load that is modeled as constant impedance, implies that the power is quadratically proportional to the voltage; in the case of the constant current, the power is directly proportional to the voltage; and when the load is modeled as a constant power, the power does not change with the voltage [27]. The ZIP coefficients [28] and the nodes for each customer class used in this study are given in Table I.

### III. IMPLEMENTATION OF VVO/CVR ALGORITHM

The VVO/CVR problem is implemented with two stages:

- Power loss minimization by distributed reactive power control.
- Voltage reduction by reducing the tap position of VR.

#### A. Distributed nonlinear controller design algorithm for loss minimization

Loss minimization is formulated as a nonlinear objective problem minimized by controlling the reactive power generation reference of DGs and D-STATCOMs as defined in problem formulation section.

Since the objective function represented by (1) is definitely positive, it is available Lyapunov candidate for the control of the nonlinear systems. According to nonlinear control theory, the condition for decreasing objective function is given below [29].

$$\frac{\partial f}{\partial t} = \sum_{i \in N_G} \frac{\partial f}{\partial Q_{Gi}} \frac{\partial Q_{Gi}}{\partial t} \leq 0 \quad (13)$$

To guarantee the absolute negativity of derivative term of the objective function with respect to time, the control law is designed as;

$$\frac{\partial Q_{Gi}}{\partial t} = - \frac{\partial f}{\partial Q_{Gi}} \quad (14)$$

By substituting (14) to (13);

$$\frac{\partial f}{\partial t} = - \sum_{i \in N_G} \left( \frac{\partial f}{\partial Q_{Gi}} \right)^2 \leq 0 \quad (15)$$

The control law in (14) can easily be realized using the below approximation [30],

$$\frac{\partial f}{\partial Q_{Gi}} \approx \frac{f(Q_{Gi}[k]) - f(Q_{Gi}[k-1])}{Q_{Gi}[k] - Q_{Gi}[k-1]} \quad (16)$$

It is essential to calculate the partial derivative of the objective function with respect to  $Q_{Gi}$  to improve control

accuracy, as indicated in [31],

$$\frac{\partial f}{\partial Q_{Gi}} = \frac{\partial f}{\partial V_i} \frac{\partial V_i}{\partial Q_{Gi}} = \frac{\partial P_{loss}}{\partial V_i} \frac{\partial V_i}{\partial Q_{Gi}} \quad (17)$$

As shown in (17) the gradient of power loss with respect to  $Q_{Gi}$  can be obtained by the product of two terms, where the first term is;

$$\frac{\partial P_{loss}}{\partial V_i} = 2 \sum_{j=1}^n V_j Y_{ij} \cos(\theta_{ij} + \delta_{ji}) \quad (18)$$

Using the ZIP load model, the second term can be calculated from reactive power flow (3) and it is derived similar to that in [22],[29],[31].

Second term is calculated as follows:

$$\frac{\partial V_i}{\partial Q_{Gi}} = \frac{V_i}{Q_{Gi} - Q_{Li} - V_i^2 B_{ii} + 2V_i^2 Z_q + V_i I_q} \quad (19)$$

Product of the two terms (18) and (19), the gradient of power loss can be obtained as follows:

$$\frac{\partial f}{\partial Q_{Gi}} = \frac{2V_i \sum_{j=1}^n V_j Y_{ij} \cos(\theta_{ij} + \delta_{ji})}{Q_{Gi} - Q_{Li} - V_i^2 B_{ii} + 2V_i^2 Z_q + V_i I_q} \quad (20)$$

It is clearly seen that only admittance of the lines, the ZIP load coefficients and local information, such as node voltage, present reactive power generation are needed to calculate the gradient. Global parameter of the system is not needed. (20) can be used to update the reactive power generation for power loss minimization. The derivative of  $Q_{Gi}$  can be approximated by;

$$\frac{\partial Q_{Gi}}{\partial t} \approx \frac{Q_{Gi}[k+1] - Q_{Gi}[k]}{\Delta t} \quad (21)$$

(20) can be rewritten as;

$$Q_{Gi}[k+1] = Q_{Gi}[k] + \frac{\partial Q_{Gi}}{\partial t} \Delta t \quad (22)$$

$\Delta t$  is the time interval for control setting update.

Finally, the control variable is updated according to the nonlinear controller as follows;

$$Q_{Gi}[k+1] = Q_{Gi}[k] - \frac{\partial f}{\partial Q_{Gi}} \Delta t \quad (23)$$

Agent system is adopted for distributed algorithm. Each node has been assigned to a node agent which can communicate with its neighbors and update its local information. When two nodes are connected to each other, these are considered to be neighbors. By doing so, exchange of the information regarding reactive power, voltage magnitudes and angles can be achieved. Each node agent should provide voltage magnitude and angle to the neighbors of itself by using local measurements. The agent which has reactive power sources should calculate the derivative term using (20) to update the control variable (23). The flow chart of the distributed power loss minimization is given in Fig. 1(a).

#### B. Tap reference calculation for CVR by voltage reduction at substation

Firstly, the voltages of the nodes in the distribution system are calculated from the power flow and hence the minimum node voltage (end of line voltage) is obtained. Secondly, tap sensitivity which defines the voltage variation per a step tap variation is calculated by dividing the

controllable voltage margin of VR (0.9 – 1.1 p.u.) to the number of taps. The VR employed in the simulations has steps of 0.00625 p.u. The reference tap for CVR is calculated by using the tap sensitivity and the voltage margin between minimum voltage of the distribution system and the minimum predefined voltage limit so that the minimum voltage of the system is close to the lower limit as much as possible. The flow chart of the voltage reduction algorithm is given in Fig. 1(b).

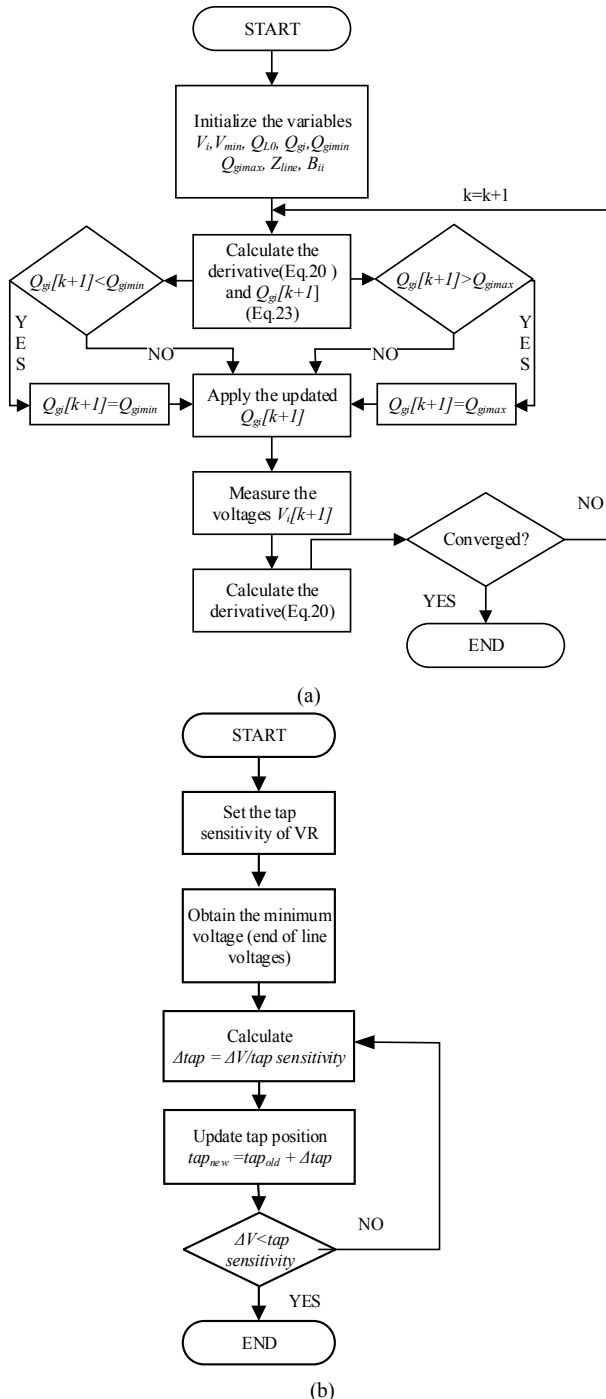


Figure 1. (a) Power loss minimization algorithm by distributed reactive power control and (b) voltage reduction algorithm

According to American National Standards Institute (ANSI) Standard C84.1 [32], the range of voltages at transformer secondary terminals is defined as  $\pm 5\%$  under normal condition. All node voltages along the feeders should be between 0.95 and 1.05 p.u. The principle of the

CVR is to reduce all voltages as close as to the minimum limit 0.95 p.u. without causing any harm to the loads by providing the all voltages within the limits, between 0.95 and 1.05 p.u. [33].

The effect of CVR can be considered as the conservation voltage regulation factor  $CVR_f$ , which is calculated as follows [33]:

$$CVR_f = \frac{\Delta P\%}{\Delta V\%} \quad (24)$$

where  $\Delta P\%$  is the percentage of demand reduction and  $\Delta V\%$  is the percentage of voltage reduction. Also, CVR factor can be calculated in terms of reactive power and energy.

#### IV. CASE STUDIES

In this work, reactive power optimization algorithm and the control of taps are implemented whereas power flow simulations are performed using OpenDSS which is the open source simulation package developed by EPRI [34]. The day is divided into 24 intervals each of an hour duration as the measuring instruments such as smart meters would update the equipment measurements and status once every hour [25].

##### A. IEEE 13 node test system feeder

In order to analyze the VVO/CVR impact on distribution systems, the proposed distributed reactive power flow control based approach has been applied to the IEEE-13 bus test feeder [35] with voltage dependent load (ZIP load model). Fig. 2 shows the single line diagram of the IEEE 13 node test system feeder. The IEEE 13-node test system consists of 13 buses interconnected by means of 10 lines which consist of overhead and underground with a variety of phasing (total 23 lines), 1 switch, 1 main transformer  $\Delta$  - Y to 115/4.16 kV at substation, 1 in line transformer to 4.16/0.480 kV, 1 voltage regulator transformers consisting of three single phase with 32 taps and two shunt capacitor banks which are 3 phase capacitor banks (600 kVAR) and 1 one phase capacitor bank (100 kVAR), unbalanced spot and distributed loads. The total active and reactive power demands of the system are 3466 kW and 2102 kVAr, respectively. The system data are taken from [36]. The voltage magnitude limits of the substation and load buses are between 0.9 - 1.1 p.u. and 0.95 - 1.05 p.u. according to the standards, respectively. The transformer tap settings have 32 discrete steps of 0.625% and can be varied in the range 0.9 - 1.1 p.u.

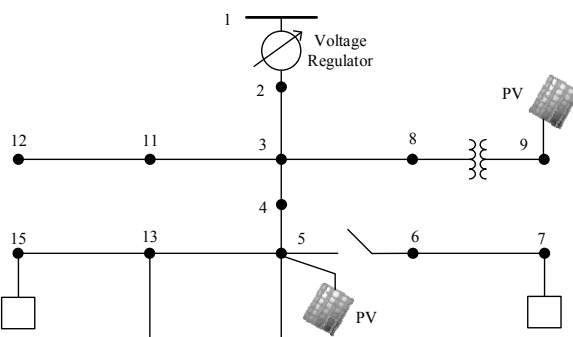


Figure 2. IEEE 13 node test system feeder [35] with DGs and D-STATCOMs

The loads of the system have been divided into three different customers: residential, commercial and industrial (see Table I). Fig. 3 illustrates the daily load demand profile for a residential customer [28], a commercial [28] and industrial user [37] and also daily PV profile [38]. It can be seen that the typical residential customer peaks at the time 20.00 of the day whereas the commercial and industrial customer peak at the time 13.00 and 11.00 of the day, respectively.

It should be noted that the distributed load between nodes is located in the middle of the line and the particular node of the distributed load is also numbered. In addition, the test system is renumbered for ease of simulation implementations.

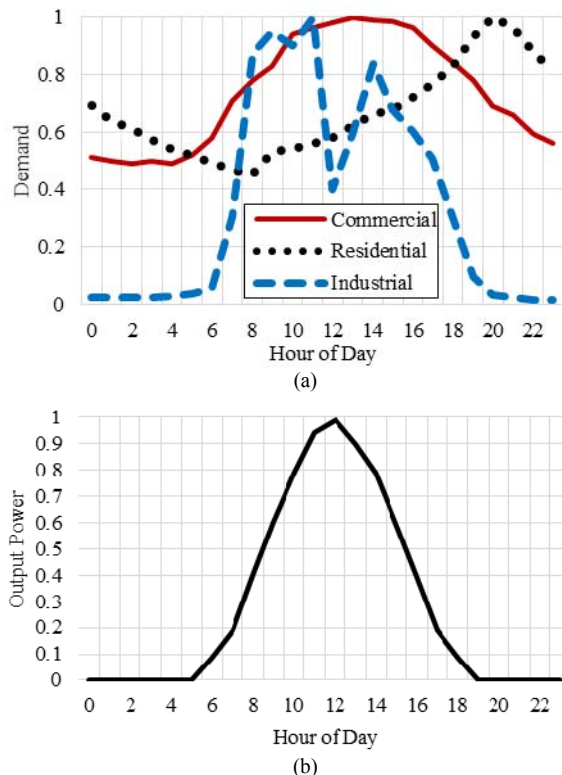


Figure 3. (a) The 24-h load profile for residential, commercial and industrial customer and (b) active power output of PV

In order to apply VVO/CVR control strategies, some modifications have been made on the original system by adding D-STATCOMs as reactive power sources and two PVs as DGs to apply the CVR effectively. PVs are located at nodes 5 and 9 with 100 kW capacity connected through the 125 kVA capacity of smart inverters per phase. Also, the capacitor banks on the original system at nodes 7 and 15 are replaced with D-STATCOMs which have the capacity of 200 kVAr per phase.

#### B. Cases

In order to demonstrate a two stages VVO/CVR algorithm in reducing the power demand without violating voltage limits, three different case studies are conducted with 24 hours load profile and different load types as follows:

The first case corresponds to base case (BC) which is obtained by using the original IEEE 13 node test system feeder with the ZIP load. The devices are operated under conventional control. VR is controlled by line drop compensation and the capacitor banks at nodes 7 and 15 are

fixed as in original IEEE 13 node test system. This case is tested without (BC) and with PV (BCpv) installed at nodes 5 and 9. PVs are operated under unity power factor.

Case 2 is the CVR case in which the fixed capacitor is replaced by the D-STATCOMs as adjustable reactive power sources. The reactive power references of D-STATCOMs are calculated by loss minimization algorithm and tap position is calculated based on tap reference calculation algorithm. This case is also tested without (CVR2) and with PV (CVR2pv) installed at nodes 5 and 9. PVs are operated under unity power factor in this case.

Case 3 (CVR3pv); PVs can be operated at different power factor, in which PV inverters inject both active and reactive power and also D-STATCOMs and reactive power output of PV inverters are controlled by distributed loss minimization algorithm.

In Table II, ‘ $P_{loss}$  (Power loss minimization)’ means that reactive power sources are used for power loss minimization without changing tap and voltage reduction. ‘CVR’ represents the full algorithm after reducing tap by calculating tap reference.

TABLE II. DAILY ENERGY LOSSES FOR ALL CASES

|               | Energy losses (kWh) |        |            |
|---------------|---------------------|--------|------------|
|               | BC                  | BCpv   | $P_{loss}$ |
| <b>CVR</b>    | 878.46              | 870.66 |            |
| <b>CVR2</b>   | 898.04              | 870.66 |            |
| <b>CVR2pv</b> | 776.25              | 755.06 |            |
| <b>CVR3pv</b> | 747.80              | 701.32 |            |

As can be clearly seen from Table II that after the power loss optimization algorithm is applied, energy losses are decreased for all cases from 878.46 kWh to 870.66 kWh in case CVR2, from 765.49 to 755.06 kWh and 701.32 kWh in case CVR2pv and CVR3pv respectively.

After the voltage reduction algorithm is applied, energy losses are increased due to the voltage reduction. Because of the industrial loads which are constant power loads, when the voltage decreases, the current drawn by the industrial loads increases.

After VVO/CVR algorithm is applied, the energy drawn through substation is decreased for all cases as given in Table III. It can be seen that maximum daily energy reduction is achieved in case CVR3pv which is using the reactive power capability of PVs and D-STATCOMs as a reactive power sources. Also, the highest energy reduction occurs in CVR3pv by 3.06% compared to BC.

TABLE III. DAILY SUBSTATION ENERGY AND REDUCTION IN ENERGY W.R.T. BASE CASE FOR ALL CASES

|               | Substation Energy (kWh) | Reduction% |
|---------------|-------------------------|------------|
| <b>BC</b>     | 49832.34                |            |
| <b>BCpv</b>   | 45548.87                |            |
| <b>CVR2</b>   | 48507.03                | 2.66%      |
| <b>CVR2pv</b> | 44216.2                 | 2.926%     |
| <b>CVR3pv</b> | 44155.94                | 3.06%      |

In Table IV, the time and the percent of maximum demand reduction and demand reduction in peak demand are presented. Also, CVR factor of active power at these times are calculated. Maximum CVR factor was obtained in case CVR3pv. The reduction in demand and CVR factor are time variant and depend on the load type due to the percentage variations of residential, commercial and industrial loads. However, the peak demands are decreased

by 1.98%, 2.56% and 2.58% for case CVR2, CVR2pv and CVR3pv respectively. By comparing the case CVR2pv and CVR3pv, it is seen that the reduction and  $CVR_f$  factor are raised by using the reactive capability of smart inverter of PVs.

TABLE IV. MAXIMUM DEMAND REDUCTION, DEMAND REDUCTION AT PEAK DEMAND AND CVR FACTOR

| Case   | Time  | $\Delta P\%$ | $CVR_f$ |
|--------|-------|--------------|---------|
| CVR2   | 3.00  | 3.587        | 0.64    |
|        | 14.00 | 1.983        | 0.396   |
| CVR2pv | 12.00 | 4.05         | 0.69    |
|        | 17.00 | 2.564        | 0.49    |
| CVR3pv | 6.00  | 4.05         | 0.695   |
|        | 17.00 | 2.583        | 0.496   |

In Fig. 4, the peak demand occurs at time 14:00 and 17:00 for BC, CVR2 and BCpv, CVR2pv and CVR3pv respectively. Fig. 4 shows that the peak demand is reduced by applying the VVO/CVR algorithm.

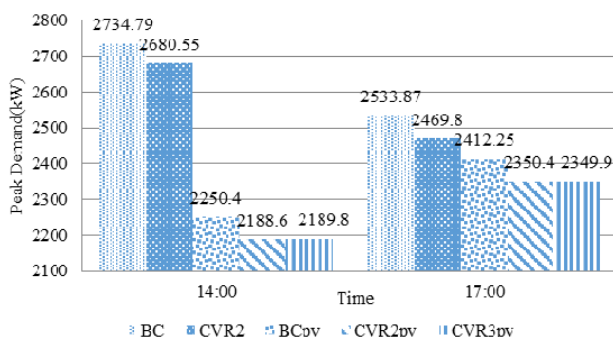


Figure 4. Peak demand

In voltage profile figures (Fig. 5 and Fig. 6), 'BC' denotes the voltage profile without any changes, under conventional control (Base Case), 'Ploss' means that reactive power sources are used for power loss minimization without changing tap and voltage reduction. CVR represents the voltage profile after reducing tap by calculating tap reference.

As can be seen from Fig. 5 and Fig. 6 that the power loss minimization algorithm does not only minimize the losses but also flatten the voltage profile by using reactive power sources such as D-STATCOM and reactive power support of smart inverter of PV. Secondly, the voltage is reduced down to lower acceptable limit by reducing the tap of VR based on tap reference calculation after power loss minimization algorithm is implemented.

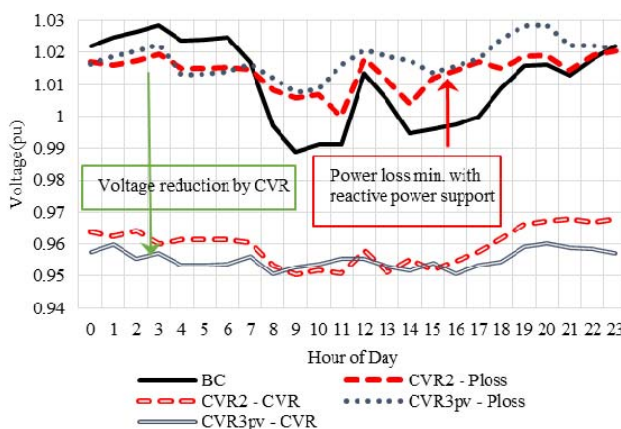


Figure 5. Daily voltage profile of node 7 - phase C

In Fig. 5 and Fig. 6, it is clearly seen that the more flatten voltage profile can be achieved by reactive power sources, and more voltage reduction can be obtained. The more voltage reduction or low voltage profile within the limit provides more energy savings and reduction in power demand.

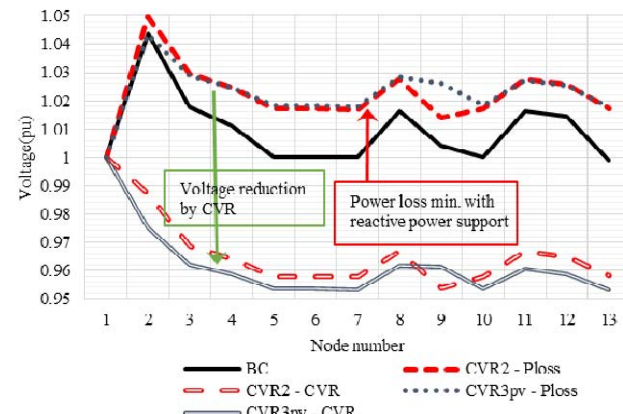


Figure 6. Phase C voltage profile of nodes at time 17:00

In Fig. 5 and Fig. 6, the voltage profile is shown before tap reference changes are applied after just power loss minimization algorithm is applied. Case CVR3pv has the most flatten voltage profile due to the more reactive power support from more nodes: the nodes installed D-STATCOM and PV. This is because the reactive power injection capability of PV inverter is used in CVR3pv case in addition to other reactive power sources. It provides the lowest voltage profile among other cases after voltage reduction is applied. Hence the lower voltage profile leads to more reduction in demand and energy savings can be seen from the figures and tables.

The reactive power outputs of D-STATCOMs are shown in Fig. 7. Reactive power output of B phase is less than the other phases due to light loading of Phase B.

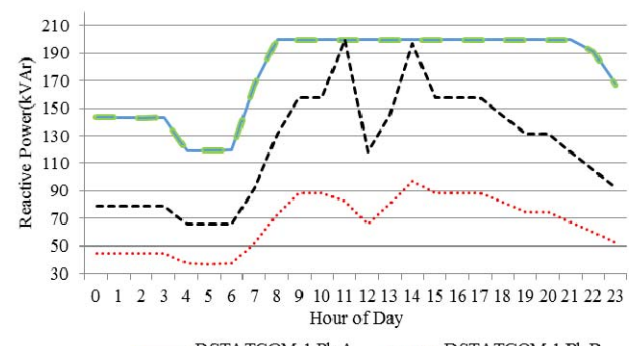


Figure 7. Reactive power output of D-STATCOMs for case CVR3pv

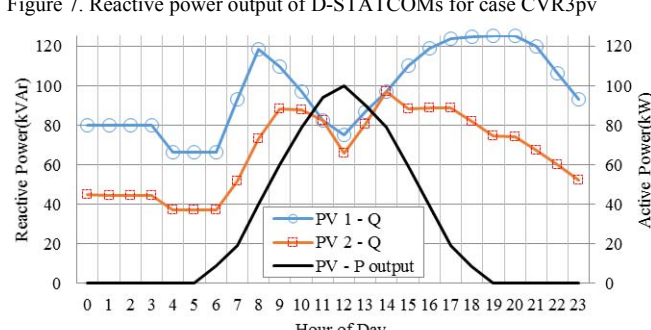


Figure 8. Active and reactive power output of PVs for case CVR3pv

Fig. 8 demonstrates the active power and the reactive power output of smart inverter of PVs. It can be seen that when the active power outputs of PVs are maximum at time 12.00, the reactive power outputs are decreased due to the apparent power limit of smart inverter (6).

Fig. 9 shows the total demand which flows through the substation over 24 hours. It can be clearly seen that the substation power is the lowest in case CVR3pv. Hence, case CVR3pv (CVR with reactive power support of DGs) gives the higher reduction in power and energy as shown in Fig. 10 due to injecting the reactive power to the system by DGs.

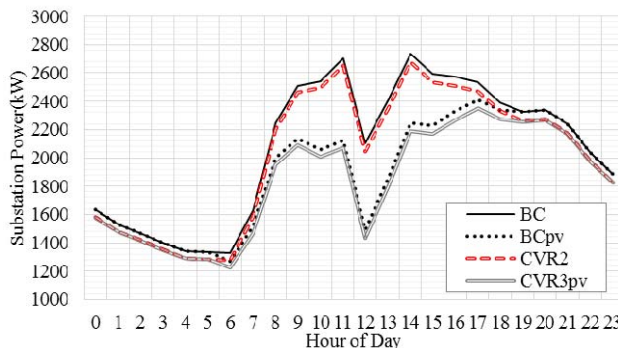


Figure 9. Daily substation power

Minimum and maximum demand reduction are obtained at time 8:00 and 20:00 as in Fig. 10. At time 8:00, the distribution system contains the massive amount industrial loads with compared to residential and commercial loads. At time 20:00, a large amount of the load in the system is residential and commercial customers which have higher voltage sensitivities with respect to power.

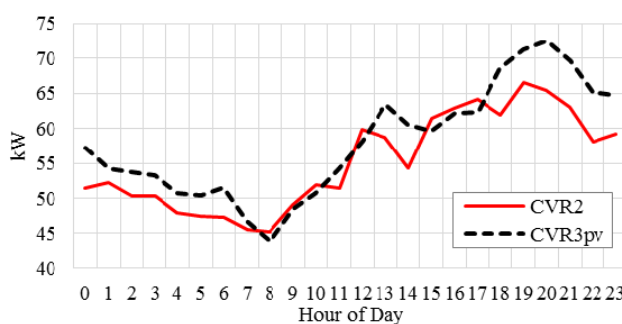


Figure 10. Demand reduction for case CVR2 and CVR3pv

Therefore, the CVR behavior of each customer may vary depending on the load type. Hence, the energy and power of residential and commercial loads compared to the industrial loads are reduced by decreasing the voltage [23].

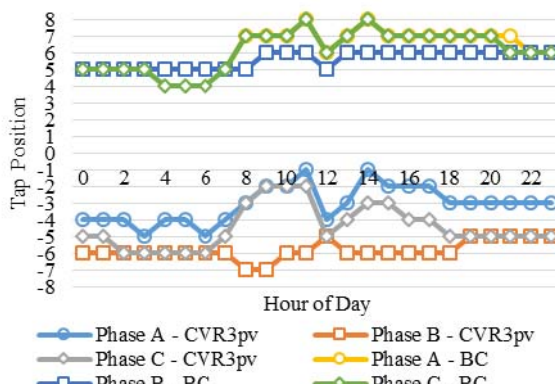


Figure 11. Tap Position of VR for base case and CVR3pv

The tap positions of VR are given in Fig. 11 for BC and CVR3pv, the reduction in the tap positions of VR can be seen by voltage reduction to implement CVR.

It can be seen from Fig. 12 that tap positions for BC and CVR3pv are lower than for case CVR2pv because case CVR3pv has more opportunity to lower the tap due to the presence of the reactive power injection of DGs.

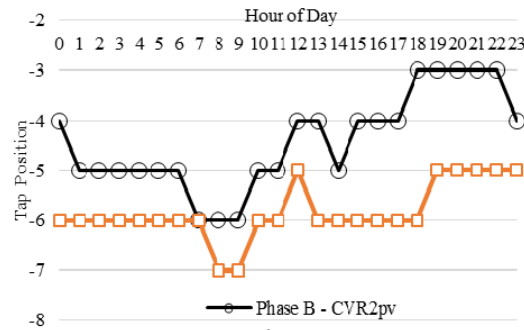


Figure 12. Tap position for case CVR2pv and CVR3pv

## V. CONCLUSION

This paper proposes a two stage VVO/CVR algorithm based on a distributed reactive power algorithm in unbalanced power distribution systems. Firstly, the reactive power reference of D-STATCOM and DGs are obtained by distributed algorithm to minimize power loss and flatten the voltage profile. Secondly the tap position of VR is reduced down to the minimum limits to achieve CVR. The algorithm is tested on IEEE 13 node test system regarding unbalanced loading with voltage dependent load model and unbalance line configuration with mutual coupling between lines.

By integration and reactive power capability of DGs (PVs), the voltage profile along the feeder is not only improved, but more energy reduction and economic savings are obtained, due to allowance to more voltage reduction. Therefore, it can be concluded that including reactive power support of DGs in VVO/CVR operation, more energy savings and power loss minimization are obtained if the devices are properly controlled.

## REFERENCES

- [1] S. Civanlar and J. J. Grainger, "Volt/Var Control on Distribution Systems with Lateral Branches Using Shunt Capacitors and Voltage Regulators Part II: The Solution Method," *IEEE Transactions on Power Apparatus and Systems*, vol. PAS-104, no. 11, pp. 3284–3290, Nov. 1985. doi:10.1109/tpas.1985.318843
- [2] H. Ahmadi, J. R. Marti, and H. W. Dommel, "A Framework for Volt-VAR Optimization in Distribution Systems," *IEEE Transactions on Smart Grid*, vol. 6, no. 3, pp. 1473–1483, May 2015. doi:10.1109/tsg.2014.2374613
- [3] S. Singh, A. K. Thakur, S. P. Singh, "Energy savings in distribution network with smart grid-enabled CVR and distributed generation," in Proc. National Power Systems Conference, India, 2016. doi:10.1109/npsc.2016.7858959
- [4] J. Sandraz et al., "Energy and Economic Impacts of the Application of CVR in Heavily Meshed Secondary Distribution Networks," *IEEE Transactions on Power Delivery*, vol. 29, no. 4, pp. 1692–1700, Aug. 2014. doi:10.1109/tpwrd.2014.2304501
- [5] M. A. Peskin, P. W. Powell, E. J. Hall, "Conservation voltage reduction with feedback from advanced metering infrastructure," in Proc. IEEE Power Eng. Soc. Transm. Distrib. Conf., Florida, 2012, pp. 1–8. doi:10.1109/tcd.2012.6281644
- [6] R. H. F. Kennedy, Barry W, "Conservation voltage reduction (CVR) at Snohomish County PUD," *IEEE Trans. Power Syst.*, vol. 6, no. 3, pp. 986–998, August 1991. doi:10.1109/59.119238

- [7] W. Ellens, A. Berry, S. West, "A quantification of the energy savings by conservation voltage reduction," in Proc. IEEE Int. Conf. Power Syst. Technol., New Zealand, 2012, pp. 1–6. doi:10.1109/powercon.2012.6401391
- [8] A. Bokhari et al., "Experimental Determination of the ZIP Coefficients for Modern Residential, Commercial, and Industrial Loads," IEEE Transactions on Power Delivery, vol. 29, no. 3, pp. 1372–1381, Jun. 2014. doi:10.1109/tpwrd.2013.2285096
- [9] D. M. Lauria, "Conservation Voltage Reduction (CVR) at Northeast Utilities," IEEE Power Engineering Review, vol. PER-7, no. 10, pp. 58–59, Oct. 1987. doi:10.1109/mper.1987.5526758
- [10] S. Lefebvre, et al., "Measuring the efficiency of voltage reduction at Hydro-Quebec distribution," in Proc. IEEE Power Energy Soc. Gen. Meet. Convers. Deliv. Electr. Energy 21st Century, Pittsburgh, 2008, pp. 1–7. doi:10.1109/pes.2008.4596511
- [11] S. M. Moghaddas-Tafreshi and E. Mashhour, "Distributed generation modeling for power flow studies and a three-phase unbalanced power flow solution for radial distribution systems considering distributed generation," Electric Power Systems Research, vol. 79, no. 4, pp. 680–686, Apr. 2009. doi:10.1016/j.epsr.2008.10.003
- [12] P. Włodarczyk, A. Sumper, and M. Cruz, "Voltage Control of Distribution Grids with Multi-Microgrids Using Reactive Power Management," Advances in Electrical and Computer Engineering, vol. 15, no. 1, pp. 83–88, 2015. doi:10.4316/aece.2015.01012
- [13] A. Bokhari et al., "Combined Effect of CVR and DG Penetration in the Voltage Profile of Low-Voltage Secondary Distribution Networks," IEEE Transactions on Power Delivery, vol. 31, no. 1, pp. 286–293, Feb. 2016. doi:10.1109/tpwrd.2015.2422308
- [14] Standards Coordinating Committee 21, "IEEE standard for interconnecting distributed resources with electric power systems," Technology, IEEE, New York, July 2003. doi:10.1109/IEEESTD.2003.94285
- [15] IEEE Standards Coordinating Committee 21, "IEEE standard for interconnecting distributed resources with electric power systems amendment 1," IEEE, New York, pp. 1–207, May 2014. doi:10.1109/IEEESTD.2014.6818982
- [16] A. Cagnano, E. De Tuglie, M. Liserre, and R. A. Mastromauro, "Online Optimal Reactive Power Control Strategy of PV Inverters," IEEE Transactions on Industrial Electronics, vol. 58, no. 10, pp. 4549–4558, Oct. 2011. doi:10.1109/tie.2011.2116757
- [17] R. J. Bravo, S. A. Robles, T. Bialek, "VAr support from solar PV inverters," in Proc. 40th IEEE Photovoltaic Specialists Conference, Colorado, 2014, pp.2672–2676. doi:10.1109/pvsc.2014.6925479
- [18] B. Bakhshideh Zad, H. Hasanzadeh, J. Lobry, and F. Vallée, "Optimal reactive power control of DGs for voltage regulation of MV distribution systems using sensitivity analysis method and PSO algorithm," International Journal of Electrical Power & Energy Systems, vol. 68, pp. 52–60, Jun. 2015. doi:10.1016/j.ijepes.2014.12.046
- [19] Z. Shen, M. E. Baran, "Gradient based centralized optimal Volt/Var control strategy for smart distribution system," in Proc. IEEE PES Innovative Smart Grid Technologies (ISGT), Washington, 2013, pp. 1–6. doi:10.1109/isgt.2013.6497865
- [20] A. Castillo, P. Lipka, J.-P. Watson, S. S. Oren, and R. P. O'Neill, "A successive linear programming approach to solving the IV-ACOPF," IEEE Transactions on Power Systems, vol. 31, no. 4, pp. 2752–2763, Jul. 2016. doi:10.1109/tpwrs.2015.2487042
- [21] A. Padilha-Feltrin, D. A. Quijano Rodezno, and J. R. S. Mantovani, "Volt-VAR Multibjective Optimization to Peak-Load Relief and Energy Efficiency in Distribution Networks," IEEE Transactions on Power Delivery, vol. 30, no. 2, pp. 618–626, Apr. 2015. doi:10.1109/tpwrd.2014.2336598
- [22] W. Zhang, W. Liu, X. Wang, L. Liu, and F. Ferrese, "Distributed Multiple Agent System Based Online Optimal Reactive Power Control for Smart Grids," IEEE Transactions on Smart Grid, vol. 5, no. 5, pp. 2421–2431, Sep. 2014. doi:10.1109/tsg.2014.2327478
- [23] Z. Wang and J. Wang, "Review on Implementation and Assessment of Conservation Voltage Reduction," IEEE Transactions on Power Systems, vol. 29, no. 3, pp. 1306–1315, May 2014. doi:10.1109/tpwrs.2013.2288518
- [24] H. J. Liu, T. J. Overbye, "Smart-grid-enabled distributed reactive power support with conservation voltage reduction," in Proc. IEEE Power Energy Conf. Illinois, 2014, pp. 1–5. doi:10.1109/peci.2014.6804573
- [25] W. H. Kersting and W. H. Phillips, "Distribution feeder line models," IEEE Transactions on Industry Applications, vol. 31, no. 4, pp. 715–720, Aug. 1995. doi:10.1109/28.395276
- [26] Y. Xu, W. Zhang, W. Liu, and F. Ferrese, "Multiagent-Based Reinforcement Learning for Optimal Reactive Power Dispatch," IEEE Transactions on Systems, Man, and Cybernetics, Part C (Applications and Reviews), vol. 42, no. 6, pp. 1742–1751, Nov. 2012. doi:10.1109/tsmc.2012.2218596
- [27] "Load representation for dynamic performance analysis (of power systems)," IEEE Transactions on Power Systems, vol. 8, no. 2, pp. 472–482, May 1993. doi:10.1109/59.260837
- [28] M. Diaz-Aguila et al., "Field-Validated Load Model for the Analysis of CVR in Distribution Secondary Networks: Energy Conservation," IEEE Transactions on Power Delivery, vol. 28, no. 4, pp. 2428–2436, Oct. 2013. doi:10.1109/tpwrd.2013.2271095
- [29] I. Khan, Z. Li, Y. Xu, and W. Gu, "Distributed control algorithm for optimal reactive power control in power grids," International Journal of Electrical Power & Energy Systems, vol. 83, pp. 505–513, Dec. 2016. doi:10.1016/j.ijepes.2016.04.004
- [30] C. Ahn and H. Peng, "Decentralized Voltage Control to Minimize Distribution Power Loss of Microgrids," IEEE Transactions on Smart Grid, vol. 4, no. 3, pp. 1297–1304, Sep. 2013. doi:10.1109/tsg.2013.2248174
- [31] A. Makanouninejad and Z. Qu, "Realizing Unified Microgrid Voltage Profile and Loss Minimization: A Cooperative Distributed Optimization and Control Approach," IEEE Transactions on Smart Grid, vol. 5, no. 4, pp. 1621–1630, Jul. 2014. doi:10.1109/tsg.2014.2308541
- [32] ANSI C84.1-2006, "American National Standard for Electric Power Systems and Equipment," Natl. Electr. Manuf. Assoc., pp. 1–24, Dec. 2006.
- [33] Z. Wang, M. Begovic, and J. Wang, "Analysis of conservation voltage reduction effects based on multistage SVR and stochastic process," IEEE Transactions on Smart Grid, vol. 5, no. 1, pp. 431–439, 2014. doi:10.1109/pesgm.2014.6939835
- [34] R. C. Dugan, T. E. McDermott, "An open source platform for collaborating on smart grid research," in Proc. IEEE Power Energy Soc. Gen. Meet., Detroit, 2011, pp. 1–7. doi:10.1109/pes.2011.6039829
- [35] W. H. Kersting, "Radial distribution test feeders," IEEE Transactions on Power Systems, vol. 6, no. 3, pp. 975–985, Aug. 1991. doi:10.1109/59.119237
- [36] IEEE 13 node test feeder, IEEE Power Engineering Society, 2010, p. 11.
- [37] J. A. Jardini, C. M. V. Tahan, M. R. Gouvea, S. U. Ahn, and F. M. Figueiredo, "Daily load profiles for residential, commercial and industrial low voltage consumers," IEEE Transactions on Power Delivery, vol. 15, no. 1, pp. 375–380, Jan. 2000. doi:10.1109/61.847276
- [38] K. M. A. Ali, R. David, "Adaptive multi-objective optimization for power loss minimization and voltage regulation in distribution systems," in Proc. Eighteenth International Middle East Power Systems Conference, Egypt, 2016, pp. 2–7. doi:10.1109/mepcon.2016.7836949